On the Circuit Solutions towards Broadband and High-Capability Piezoelectric Energy Harvesting Systems

Bao Zhao and Junrui Liang

School of Information Science and Technology, ShanghaiTech University
No. 393, Middle Huaxia Road, Pudong, Shanghai 201210, China

ABSTRACT

In the studies of piezoelectric energy harvesting (PEH) systems, literature has shown that the circuit solution has a significant effect towards the enhancement of energy harvesting capability under resonance. Some studies started to investigate its bandwidth-broadening effect recently. This paper provides a comprehensive comparison on the impact of circuit solutions towards the broadband and high-capability energy harvesting. The comparison is intuitively presented based on the equivalent impedance model. The joint dynamics and harvested power of the PEH systems using different interface circuits are thoroughly discussed. Simulation and experiments show good agreement with the analysis. It has been proved that, within the existing circuit solutions, the currently introduced phase-variable synchronized parallel triple bias-flip (PV-P-S3BF) circuit provides the most extensive span of electrically induced damping (resistive component) and electrically induced stiffness/mass (reactive component). By tuning the values of the two equivalent impedance parts in operation, the tasks of harvesting capability enhancement and bandwidth broadening can be simultaneously made by using PV-P-S3BF.

Keywords: Piezoelectric energy harvesting, broadband, interface circuit, impedance modeling

1. INTRODUCTION

The piezoelectric energy harvesting (PEH) technology converts the ambient kinetic energy into useful electricity, such that to enable some highly distributed devices in the wireless sensor networks (WSNs), which operate in vibrational environments, to become energy-self-sufficient. The two most significant research emphases for the PEH solutions are:

1. to enhance the energy harvesting capability in resonance, and
2. to broaden the bandwidth of the harvester, in order words, to enhance the off-resonance harvesting capability.

Vibrations in practical scenarios are usually characterized as broadband excitations. On the other hand, the bandwidth of linear oscillators is confined by their mechanical quality factors, which cannot be too large for the energy harvesting purpose. Therefore, conventional linear energy harvesters are only capable for harvesting energy from narrow-band vibrations.

The previous studies have shown that the first target on harvesting capability enhancement can be achieved through the power conditioning circuit designs.[1,2] Most power conditioning circuits are derived based on the synchronized switch actions, which manipulate the piezoelectric voltage at its extreme points. By doing this, the energy harvesting capability can be enhanced by several folds.[3] Shu et al.[4] have pointed out that, by using the synchronized switch circuit solutions, a weakly coupled PEH system might become a moderately or strongly coupled system. The second target on bandwidth broadening was mostly achieved through mechanical designs as introduced in literature.[5] The most investigated solutions include: the combination of different linear vibrators towards a broadband system; vibration modes redesign by appending auxiliary structures; and adding the nonlinear mechanical monostable or bistable mechanism to force the vibrator step out of its linear range. In general, compared to the mechanical designs, the existing circuit solutions have played a more significant role on energy harvesting capability enhancement; its bandwidth broadening effect was less attractive. The reason is the

Corresponding author: Junrui Liang. E-mail: liangjr@shanghaitech.edu.cn.

Active and Passive Smart Structures and Integrated Systems XII, edited by Alper Erturk, Jae-Hung Han,
Proc. of SPIE Vol. 10595, 105950E · © 2018 SPIE · CCC code: 0277-786X/18/$18 · doi: 10.1117/12.2296333

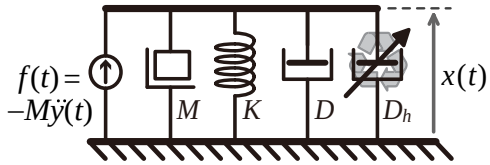

Figure 1. The early conceptual schematic model of an kinetic energy harvester.[11]

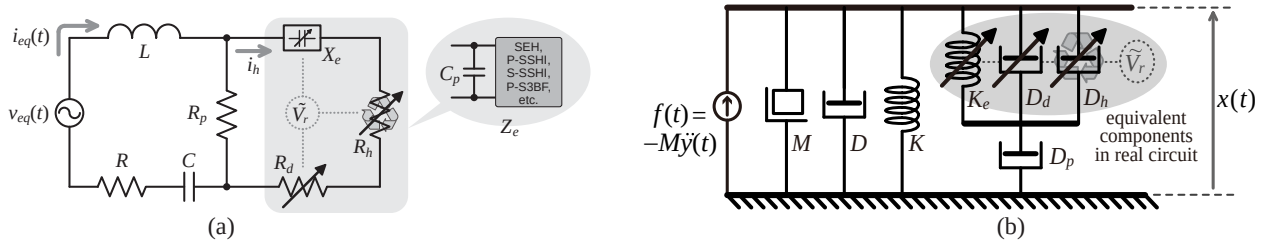

Figure 2. The electrical and mechanical equivalent models of a PEH system using practical single-variable tunable harvesting circuits.[12] (a) The equivalent impedance model. (b) The responding equivalent mechanical schematic.

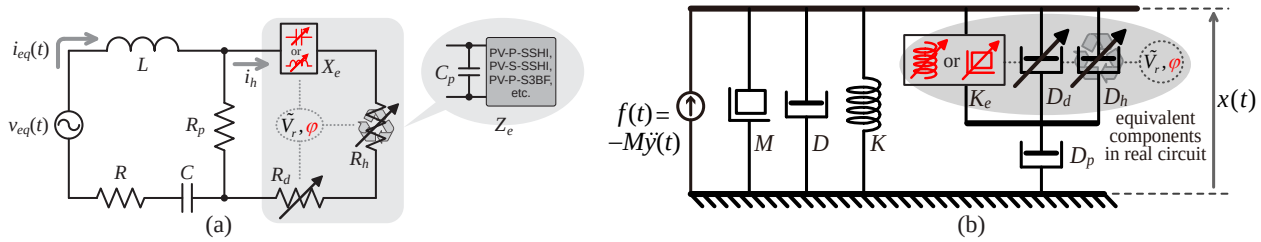

Figure 3. The electrical and mechanical equivalent models of a PEH system using practical double-variable tunable harvesting circuits. (a) The equivalent impedance model. (b) The responding equivalent mechanical schematic.

weakly or moderately coupling feature of most piezoelectric structures. Without a strong reverse piezoelectric coupling effect, the connected interface circuit has little to do with the mechanical structure.

Even the bandwidth broadening effect produced by the interface circuit was less significant, some studies have already initiated the investigations on the circuit contribution towards broader bandwidth for PEH systems. The electrical-to-mechanical interference depends on the coupling intensity and the harvesting capability of the selected interface circuit. Wu et al.[6] changed the resonant frequency by connecting different capacitors in parallel to the piezoelectric element; the effect was not significant, because such connection will further lower the coupling factor of the system. The synchronized switch harvesting on inductor (SSHI) solutions were regarded as a milestone for PEH enhancement; in the meanwhile, they also broaden the harvesting bandwidth by introducing stronger electrically induced damping effect.[3,4] Recently, some solutions investigated how to enhance the off-resonance performance by introducing a switching phase variance (lead or lag) in SCE,[7] SSHI,[8] or P-S3BF.[9] Such technologies are referred to as phase-variable SCE (PV-SCE), PV-SSHI, and PV-P-S3BF in short in the following part of this paper.

Regarding the new research trend on electrically tunable broadband PEH systems, this paper provides a comparison and exploration on the bandwidth broadening effect of different PEH interface circuits, in particular, with an emphasis on the newly introduced phase-variable synchronized switching circuits. Besides the existing circuit solutions, we also study the newly implemented phase-variable parallel triple synchronized bias-flip (PV-P-S3BF) circuit.[9] By introducing the synchronized switching phase as the second tunable variable to the P-S3BF,[10] the PV-P-S3BF might better realize the dual tasks of higher energy harvesting capability and broader harvesting bandwidth simultaneously.

2. SYSTEM MODEL

Fig. 1 shows the early conceptual model of a linear kinetic energy harvester, which was introduced by Williams and Yates in 1996.[11] Such model has defined the dynamic effect of an energy harvesting circuit as, and only as, the electrically induced damping, i.e., D_h in Fig. 1. It was assumed that all the removed energy is recycled into useful electricity and the removal of kinetic energy from vibration causes structural damping. Based on such theoretical guidance, a large research effort has focused on how to increase the electrically induced damping.[2] However, later studies have shown that such conceptual model is too simple to account for the detailed electrically induced dynamics of practical PEH interface circuits.[12–14] Such simple model without considering the electrically induced mass/stiffness has also confined our imagination towards frequency tuning in an electrical way. Given the insufficiency of the conventional conceptual model, Liang et al.[12–14] have proposed a more general dynamic model for the kinetic energy harvesting systems, which is shown in either mechanical or electrical domains, as shown in Fig. 2. For PEH systems, the insertion of piezoelectric element first adds an additional stiffness (short-circuit stiffness) K_{sc} to the structure. In addition, no matter what interface circuit is used for the energy harvesting purpose, the ac-to-dc power conditioning generally induces three dynamic components to the vibrating system: the electrically induced stiffness K_e, the dissipative damping D_d, and the regenerative (energy harvesting) damping D_h, as shown in Fig. 2(b). The parameter $\tilde{V}_r$ in the figure represents the non-dimensional rectified voltage, which controls the values of three dynamic components. D_p connecting in series to the three components represents the effect of dielectric loss in the piezoelectric element.[12]

As we can see from the linkages between $\tilde{V}_r$ and the three electrically induced components, tuning the circuit parameter can change not only the dissipative damping and regenerative damping, whose gross effect is the electrically induced damping, but also the electrically induced stiffness/mass (negative or positive reactive component). The latter electrically induced stiffness/mass has received some research interest recently.[7,8] Nevertheless, the studies were case by case regarding different energy harvesting interface circuits. A uniform model and comparison are necessary towards a comprehensive evaluation on the potential of vibration tuning using different circuit methods.

3. EQUIVALENT IMPEDANCE ANALYSIS

Since the early studies of PEH using the standard energy harvesting (SEH) interface circuit, i.e., the ac-to-dc full bridge rectifier,[15] there are dozens of circuit topologies proposed for boosting the energy harvesting capability in resonance. Boosting the energy harvesting capability, on one hand, enhances the system coupling effect; on the other, it reinforces the electrically induced mechanical intervention to the vibrating system. The most representative interface circuits for PEH include: SEH,[15] SCE,[16] SSHI,[3] SMBF,[1] etc. This paper covers the performances of these circuits, as well as their derivations after introducing the phase-variable controls, e.g., PV-SCE,[7] PV-SSHI,[8] and PV-P-S3BF.[9] Since this paper does not aim to propose any new interface circuits, readers should refer to the literature for the detailed background knowledge about the topologies, working principles, and operating waveforms of the aforementioned PEH interface circuits.

The equivalent impedance model provides a rational uniform for the comparison among the dynamics of different interface circuits.[12,13] It sets the fundamental of this comparative study. In the equivalent impedance network, as shown in Fig. 2(a), which is the counterpart of the equivalent mechanical schematic of Fig. 2(b), the series R, L, C, and $v_{eq}(t)$ components correspond to the damping D, mass M, stiffness K, and force source $f(t)$. The dissipative resistance R_d, regenerative resistance R_h, equivalent reactance X_e, piezoelectric leakage resistance R_p correspond to D_d, D_h, K_e, and D_p in Fig. 2(b). The relations in the electromechanical analogy were provided by Liang et al.,[12,13] where α_e is the force-voltage factor.

Harmonic analysis was employed for deriving the values of the electrically induced components. For the single-variable tunable circuits, the equivalent impedance expressions of SEH, parallel SSHI (P-SSHI), series SSHI (S-SSHI), and P-S3BF were developed in literature.[10,12,13] The available ranges are shown by the one-dimensional dotted, dash-dot, dashed, and dash-dot-dot lines in Fig. 4, respectively. SCE is different from the other circuits, because its equivalent impedance is a fixed number under different output dc voltage.[17] The specific impedance point of SCE is marked by the cross mark in Fig. 4. As we can observe from Fig. 4, the principles of energy harvesting capability enhancement of SCE, SSHI, and S3BF technologies are realized by increasing the "useful" real part (equivalent regenerative damping) of the equivalent impedance.

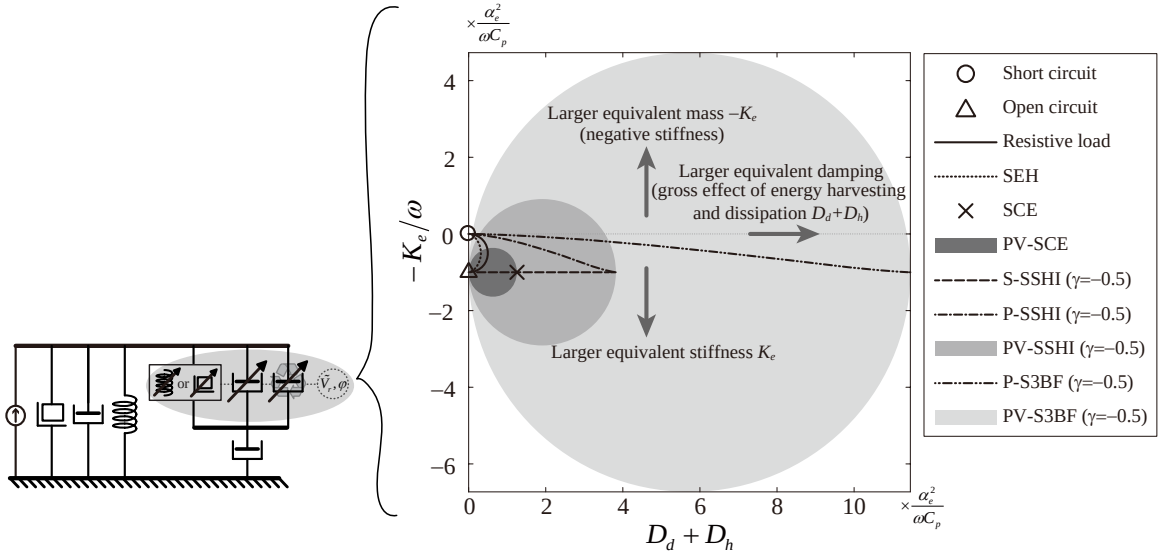

Figure 4. The attainable ranges of the electrically induced mechanical dynamics of different PEH interface circuits.

For the PV-SCE[7] and PV-SSHI (including parallel and series),[8] their equivalent impedances were not explicitly presented in the original proposals. They can be formulated according to the similar procedures developed by Liang et al.[12,13] i.e.,

1. The current i_h flowing through the three equivalent components R_h, R_d, and X_e is assumed sinusoidal.
2. The piezoelectric voltage v_p is described with a piecewise equation given the sinusoidal current and specific circuit topology and control.
3. The fundamental voltage $v_{p,f}$ is obtained by singling out the fundamental harmonic of the piezoelectric voltage v_p.
4. The equivalent impedance $Z_e = R_h + R_d + jX_e$, as a function of $\tilde{V}_r$ and φ, is derived by dividing the frequency-domain expression of $v_{p,f}$ over that of i_h, i.e., $Z_e(\tilde{V}_r, \varphi) = V_{p,f}(j\omega)/I_h(j\omega)$.

Except the different values of the three dynamic components of R_h, R_d, and X_e regarding different interface circuits in use, the analytical framework of equivalent impedance modeling[12,13] can be reused for the analysis of PEH system using any interface circuit. Taking PV-S-SSHI[8] for example, its equivalent impedance can be analyzed according to the aforementioned four procedures. For the first step, we assume sinusoidal

$$i_h(t) = I_h \sin(\omega t), \tag{1}$$

where ω is the vibration frequency, I_h is the magnitude of i_h. The piezoelectric voltage v_p in PV-S-SSHI can be formulated as follows

$$v_p(t) = V_{oc} \times \begin{cases} -\tilde{V}_M + \cos\varphi - \cos(\omega t), & \varphi \le \omega t < \pi + \varphi, \\ \tilde{V}_M - \cos\varphi - \cos(\omega t), & \pi + \varphi \le \omega t < 2\pi + \varphi, \end{cases} \tag{2}$$

where $V_{oc} = I_h/(\omega C_p)$ is the nominal open-circuit voltage, $\tilde{V}_M = V_M/V_{oc}$ is the non-dimensional end voltage of a bias-flip action. $\tilde{V}_M$ can be calculated by solving the following equations

$$\begin{cases} \tilde{V}_0 + \tilde{V}_M = \cos\varphi - \cos\theta, \\ \gamma(\tilde{V}_0 - \tilde{V}_r) = \tilde{V}_M - \tilde{V}_r, \end{cases} \tag{3}$$

where $\tilde{V}_r = V_r/V_{oc}$ is the non-dimensional rectified voltage and γ is the flipping factor in each bias-flip action. For figuring the outer boundary of the equivalent impedance of PV-S-SSHI, we can just simply let $\tilde{V}_r = 0$. Under

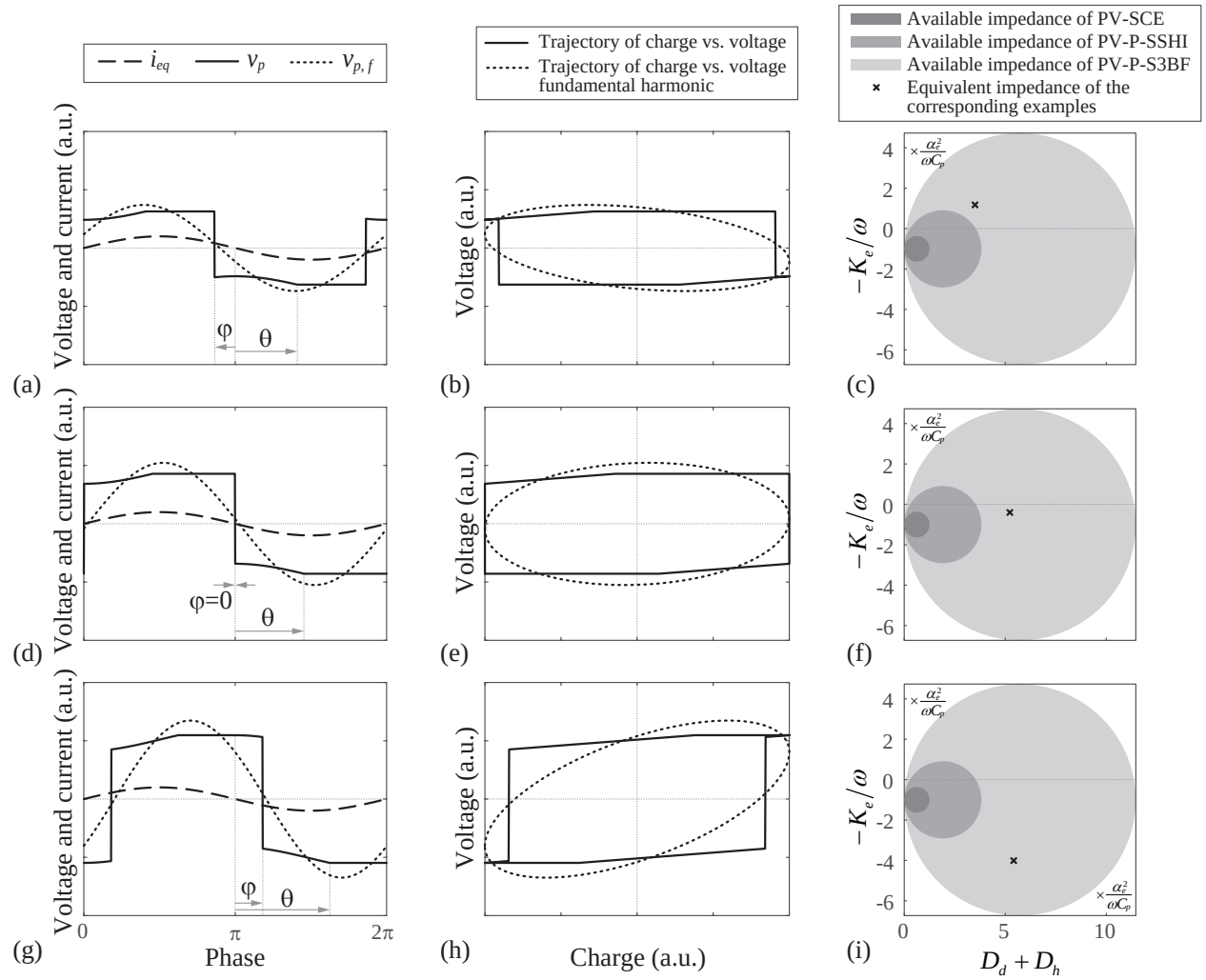

Figure 5. Waveforms and impedance pictures of PV-P-S3BF under different switching phase lag φ ($\gamma = -0.5$). (a)-(c) Phase lead switch. (d)-(f) In phase switch. (g)-(i) Phase lag switch. (a), (d), and (g) Voltage and current waveforms. (b), (e), and (h) The original work cycles and their linear approximations. (c), (f), and (i) The corresponding equivalent impedances in the impedance plane.

such condition, we can get $\tilde{V}_M = 2\gamma\cos\varphi/(1+\gamma)$. Substituting this condition into (2) and applying the harmonic analysis, we can further get the time-domain expression of the fundamental component of v_p as follows

$$v_{p,f}(t) = \frac{I_h}{\omega C_p}\left\{-\cos(\omega t) + \frac{2}{\pi}\frac{1-\gamma}{1+\gamma}\left[\sin(\omega t)\left(1+\cos 2\varphi\right) - \cos(\omega t)\sin 2\varphi\right]\right\}. \tag{4}$$

Therefore, the boundary of equivalent impedance in PV-S-SSHI can be formulated by dividing the frequency expressions of $v_{p,f}$ and i_h

$$Z_{\text{PV-SSHI,bound}}(j\omega,\varphi) = \frac{V_{p,f}(j\omega,\varphi,V_r=0)}{I_h(j\omega)} = \frac{1}{\omega C_p}\left[\frac{2}{\pi}\frac{1-\gamma}{1+\gamma} - j + \frac{2}{\pi}\frac{1-\gamma}{1+\gamma}\left(\cos 2\varphi - j\sin 2\varphi\right)\right]. \tag{5}$$

By applying the same formula, the v_p waveform in PV-P-SSHI and PV-P-S3BF can be described under two working regions.[9] Fig. 5 shows how phase lead or lag of $v_{p,f}$ (compared to i_h) are produced by varying the synchronized switch phase φ. The work cycle and equivalent impedance points in the three corresponding cases of Fig. 5(a), (d), and (g) are illustrated in Fig. 5 (b), (e), (h) and Fig. 5 (c), (f), (i), respectively. The attainable

Table 1. Specifications of the experimental PEH system.

Parameter	Value	Parameter	Value
R	57.41 kΩ	L_i	47 mH
L	2.65 kH	C_r	10 μF
C	2.70 nF	C_b	4.7 μF
C_p	57.83 nF	ω	$2\pi \times 59.8$ Hz
R_p	679.96 kΩ	Acceleration	4.9 m/s^2
γ	−0.5	MOSFET	Vishay Si4590DY

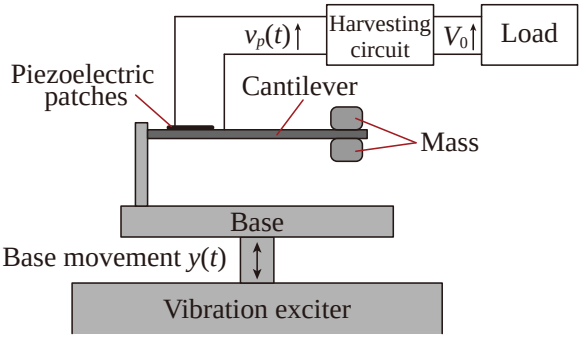

Figure 6. Experiment setup.

and tunable reactive ranges with phase-variable control are larger than that in the single-variable tunable circuits, i.e., those only switches at the zero-crossing points of the equivalent current i_h. It can be proved and summarized that the equivalent impedance of general synchronized multiple bias-flip (SMBF) solutions in the phase-variable solutions have the outer boundary expressed by the equation as follows

$$Z_{\text{PV-SMBF,bound}}(j\omega,\varphi) = \frac{1}{\omega C_p}\left[\frac{2M}{\pi}\frac{1-\gamma}{1+\gamma} - j + \frac{2M}{\pi}\frac{1-\gamma}{1+\gamma}\left(\cos 2\varphi - j\sin 2\varphi\right)\right], \tag{6}$$

where M is the number of bias-flip actions. PV-SCE is the special case when $\gamma = 0$ and $M = 1$. PV-P(S)-SSHI is the special cases when $M = 1$. PV-P-S3BF is the special case when $M = 3$. As the switch phase move from $\varphi = -\pi/2$ to $\pi/2$, it can be proved that the outer boundary of the impedance $Z_{\text{PV-SMBF,bound}}$ is in the circular shapes, whose centers locate at $\left(\frac{2M}{\pi}\frac{1-\gamma}{1+\gamma}, -j\right)$ and radius are $\frac{2M}{\pi}\frac{1-\gamma}{1+\gamma}$, respectively. The attainable two-dimensional areas of the impedances of PV-SCE, PV-P(S)-SSHI, and PV-P-S3BF are illustrated in gray and distinguished with different gradients in Fig. 4.

It can be observed that, by adopting more bias-flip actions, the attainable ranges are extended along both the real and imaginary axes. The extension of real part can enlarge the energy harvesting capability by approaching the mechanical damping intensity (usually is much larger than the electrically induced damping under weakly coupling condition); while the extension of the imaginary part might produce larger reactive component to compensate the off-resonant reactance, such that to achieve broader energy harvesting bandwidth.

4. EXPERIMENTS

Experiments are carried out for validating the energy harvesting capability and bandwidth of the PEH systems using SEH, PV-SSHI, PV-SSHI, and PV-P-S3BF interface circuits. The phase-variable switch control is implemented on a P-S3BF prototyped circuit which was developed by Zhao et al.[10] Fig. 6 shows the experiment setup. A piezoelectric cantilever, whose parameters are listed in Table 1, is excited by a shaker. An electromagnetic sensor mounted at the free end of the cantilever senses the vibration velocity for the synchronization purpose.

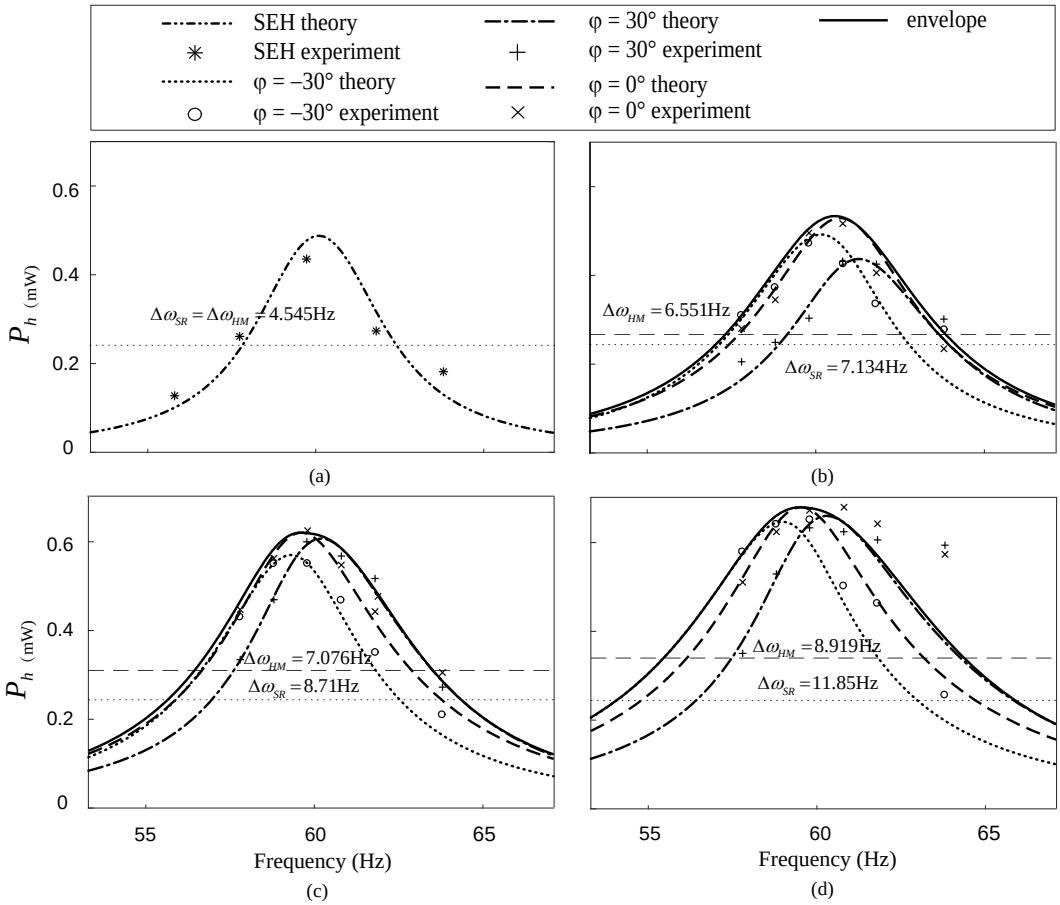

Figure 7. Harvested power P_h. (a) SEH. (b) PV-S-SSHI. (c)PV-P-SSHI. (d)PV-P-S3BF

Fig. 7 shows the maximum harvested power P_h under different vibration frequencies and switching phase lag φ in the SEH, PV-S-SSHI, PV-P-SSHI, and PV-P-S3BF cases. The $\varphi = 0$ cases are just S-SSHI, P-SSHI, and P-S3BF. The envelope of P_h in PV-S-SSHI, PV-P-SSHI, and PV-P-S3BF are shown by the solid lines. It can be observed from Fig. 7 that the half-maximum-power bandwidth $\Delta\omega_{HM}$ in PV-SSHI and PV-P-S3BF have been broadened to different extents compared to that in SEH. In particular, The harvesting bandwidth of PV-P-S3BF is 16.2% broader than that of P-S3BF and is 160.7% broader than that of SEH. On the other hand, if we take the half-maximum-power of the SEH case as a more fair reference, the SEH referenced bandwidth $\Delta\omega_{SR}$ can further show the bandwidth improvement of the advanced power conditioning circuit, compared to the standard technology. The piezoelectric patch used in this experiment is in a moderately coupled condition; therefore, the enhancement on maximum P_h is not as big as those in previous studies under weak coupling condition. In general, the simultaneous harvesting capability enhancement and bandwidth broadening by using the phase-variable topologies has been successfully validated.

5. CONCLUSION

A new circuit solution, phase-variable parallel synchronized triple bias-flip (PV-P-S3BF) interface circuit was introduced in this paper for broadening the energy harvesting bandwidth of the piezoelectric energy harvesting (PEH) systems, both the electrically induced damping and electrically induced stiffness/mass can be tuned in operation for simultaneously making the dual tasks. The working principle and impedance modeling are provided for better understanding and quantification of the electromechanical joint dynamics and harvested power by using PV-SSHI and PV-S3BF. Experiments are carried out for validating the theoretical analysis. The proposed solution and analysis provide a new insight towards the designs of broadband PEH systems.

ACKNOWLEDGMENTS

The work described in this paper was supported by the grants from National Natural Science Foundation of China (Project No. 61401277) and ShanghaiTech University (Project No. F-0203-13-003).

REFERENCES

[1] Liang, J., "Synchronized bias-flip interface circuits for piezoelectric energy harvesting enhancement: A general model and prospects," *J. Intell. Mater. Syst. Struct.* **28**(3), 339–356 (2017).

[2] Szarka, G. D., Stark, B. H., and Burrow, S. G., "Review of power conditioning for kinetic energy harvesting systems," *IEEE Trans. Power Electron.* **27**(2), 803–815 (2012).

[3] Guyomar, D., Badel, A., Lefeuvre, E., and Richard, C., "Toward energy harvesting using active materials and conversion improvement by nonlinear processing," *IEEE Trans. Ultrason. Ferroelectr. Freq. Control* **52**(4), 584–595 (2005).

[4] Shu, Y. C., Lien, I. C., and Wu, W. J., "An improved analysis of the SSHI interface in piezoelectric energy harvesting," *Smart Mater. Struct.* **16**(6), 2253–2264 (2007).

[5] Tang, L., Yang, Y., and Soh, C. K., "Toward broadband vibration-based energy harvesting," *J. Intell. Mater. Syst. Struct.* **21**(18), 1867–1897 (2010).

[6] Wu, W.-J., Chen, Y.-Y., Lee, B.-S., He, J.-J., and Peng, Y.-T., "Tunable resonant frequency power harvesting devices," *Proc.SPIE* **6169**, 6169 – 6169 – 8 (2006).

[7] Lefeuvre, E., Badel, A., Brenes, A., Seok, S., and Yoo, C.-S., "Power and frequency bandwidth improvement of piezoelectric energy harvesting devices using phase-shifted synchronous electric charge extraction interface circuit," *J. Intell. Mater. Syst. Struct.* **28**(20), 2988–2995 (2017).

[8] Hsieh, P. H., Chen, C. H., and Chen, H. C., "Improving the scavenged power of nonlinear piezoelectric energy harvesting interface at off-resonance by introducing switching delay," *IEEE Trans. Power Electron.* **30**, 3142–3155 (June 2015).

[9] Zhao, B. and Liang, J., "Phase-variable parallel synchronized triple bias flips (PV-P-S3BF) interface circuit towards broadband piezoelectric energy harvesting," in [*Proceedings of the 2018 IEEE International Symposium on Circuits and Systems (ISCAS)*], (2018).

[10] Zhao, Y. and Liang, J., "Synchronized triple bias-flip circuit for piezoelectric energy harvesting enhancement: Operation principle and experimental validation," in [*Proceedings of the 2016 IEEE Energy Conversion Congress and Exposition (ECCE)*], 1–6 (2016).

[11] Williams, C. and Yates, R., "Analysis of a micro-electric generator for microsystems," *Sens. Actuators, A* **52**(1), 8 – 11 (1996). Proceedings of the 8th International Conference on Solid-State Sensors and Actuators Eurosensors IX.

[12] Liang, J., Chung, H. S.-H., and Liao, W.-H., "Dielectric loss against piezoelectric power harvesting," *Smart Mater. Struct.* **23**(9), 092001 (2014).

[13] Liang, J. and Liao, W.-H., "Impedance modeling and analysis for piezoelectric energy harvesting systems," *IEEE/ASME Trans. Mechatron.* **17**(6), 1145–1157 (2012).

[14] Liang, J., Ge, C., and Shu, Y.-C., "Impedance modeling of electromagnetic energy harvesting system using full-wave bridge rectifier," *Proc. SPIE* **10164**, 101642N–101642N–10 (2017).

[15] Ottman, G. K., Hofmann, H. F., Bhatt, A. C., and Lesieutre, G. A., "Adaptive piezoelectric energy harvesting circuit for wireless remote power supply," *IEEE Trans. Power Electron.* **17**(5), 669–676 (2002).

[16] Lefeuvre, E., Badel, A., Richard, C., Petit, L., and Guyomar, D., "A comparison between several vibration-powered piezoelectric generators for standalone systems," *Sens. Actuators, A* **126**(2), 405–416 (2006).

[17] Chen, C., Zhao, K., and Liang, J., "Impedance analysis of piezoelectric energy harvesting system using synchronized charge extraction interface circuit," *Proc. SPIE* **10164**, 101642Q–101642Q–10 (2017).